ELSEVIER

Journal of Photochemistry and Photobiology A: Chemistry 121 (1999) 183–190

Journal of Photochemistry and Photobiology A:Chemistry

Photochemical and laser activity of 1,4-bis [ß-(2-quinoxalyl)vinyl]benzene: a new laser dye

Tarek A. Fayed*, Samy A. El-Daly, Safaa Eldin H. Etaiw

Chemistry Department, Faculty of Science, Tanta University, Tanta 31527, Egypt

Received 18 November 1998; accepted 18 December 1998

Abstract

The title diolefinic dye (BQxVB) was synthesized and its spectral characteristics were investigated in various solvents as well as microemulsions. A large solvents effect on the fluorescence maxima and quantum yields (ϕ_f) was observed. The effect of excitation wavelength on both fluorescence and photoisomerization quantum yields have been evaluated in different media and interpreted in terms of conformational equilibrium. The fluorescence quenching of BQxVB by Fe^{+3} ions was also investigated in aqueous, anionic and cationic micellar solutions. The photochemical behaviour of BQxVB in halomethane solvents (such as CH_2Cl_2, $CHCl_3$ and CCl_4) has been discussed. The dye solution in *N,N*-dimethyl formamide (DMF) lases around 460 nm upon pumping with a nitrogen laser ($\lambda_{ex} = 337.1$ nm). Energy transfer from BQxVB to rhodamine B has been studied in ethanol and the critical transfer distance has been determined.

Keywords: Solvent effect; Microemulsions; Photoisomerization; Conformational equilibrium; Laser dye; Energy transfer

1. Introduction

In recent years, there has been considerable interest in the development of dye lasers as a source of tunable radiation. The entire range of the visible spectrum can be covered, in fact, by a suitable choice of organic dye solutions, each lasing in a different region. However, for many applications it would be preferable to use a single dye solution to cover as large as possible a fraction of the visible spectrum.

Several diolefinic laser dyes, specially the aza-analogues of distyrylbenzene have been recently studied [1–6] in both homogeneous and micellar media. These dyes are highly efficient blue-emitting laser dyes with good photochemical stability in comparison with other widely used blue-emitting dyes such as coumarins. In this paper, we report the spectral and photochemical characteristics as well as the laser activity of a new diolefinic laser dye; 1,4-bis[ß-(2-quinoxalyl)-vinly]benzene (BQxVB) in different media.

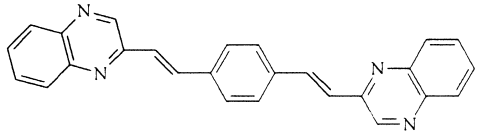

BQxVB

2. Experimental

BQxVB was prepared according to the method reported for the preparation of styrylquinoxaline [7]. The product was recrystallized twice from ethanol and characterized by elemental analysis. Calc. for $C_{26}H_{18}N_4$: C, 80.83; H, 4.66; N, 14.51 (%). Found: C, 81.40; H, 4.95; N, 13.87 (%). Also, the IR spectrum (as KBr disc) shows bands at 1640 and 1608 cm^{-1} characteristic for the ethylenic double bond, as well as a band at 970 cm^{-1} characteristic for the =C–H out of plane bending of *trans* olefins. The purity of the dye was also checked by fluorescence and UV–Vis spectral measurement. Both anionic and cationic micelles were prepared by dissolving sodium dodecylsulfate (SDS, Fluka, Puriss) and cetyltrimethyl ammonium chloride (CTAC, Kodak) in water. All solvents used in the measurements were of spectroscopic grade. The water in oil (W/O) microemulsion containing chloroform as the oil phase was prepared by mixing chloroform (oil) with water plus SDS (surfactant) plus butanol (cosurfactant) in the ratio (by weight) 37.075 : 4.308 : 4.308 : 4.308, respectively [8]. The oil in water (O/W) microemulsion was prepared by mixing the above components in the ratio 2.06 : 43.62 : 2.06 : 2.06, respectively.

Steady-state fluorescence spectra were recorded on a Perkin Elmer LS 50B luminescence spectrometer while

*Corresponding author.

1010-6030/99/$ – see front matter
PII: S1010-6030(98)00469-9

the electronic absorption spectra were recorded using a Shimadzu UV-160A spectrophotometer. Fluorescence quantum yields (ϕ_f) was measured relative to 9,10-diphenylanthracene [9] as a standard. Light intensity was measured by using ferrioxalate actinometry [10]. Continuous irradiation experiments were carried out in the same cell of a spectrofluorimeter equipped with a 10 kW xenon lamp and a monochromator. The quantum yields of *trans* ⇌ *cis* photoisomerization have been determined by the method reported previously [11]. The lasing action of BQxVB in dimethyl formamide (DMF) was monitored upon pumping with a GL-3300 nitrogen laser ($\lambda_{ex} = 337.1$ nm). A detailed description of the pumping laser source and detection system is given elsewhere [6].

3. Results and discussion

3.1. Medium effects on the spectral properties

The absorption spectra of BQxVB in three solvents of different polarities (namely cyclohexane, DMF and methanol) are shown in Fig. 1 together with the corresponding excitation and emission spectra. Table 1 shows the spectral properties and fluorescence quantum yields measured in various solvents at room temperature. BQxVB exhibits a strong absorption band in the UV region which is probably due to the allowed π–π^* transition of the conjugated ethylenic system. The π–π^* nature of the transition is supported by a large molar absorption coefficients (ε_{max} is greater than $8 \times 10^4\ M^{-1}\ cm^{-1}$) and a high fluorescence quantum yield. The excitation spectra are replica of the absorption spectra, and there is also a good mirror image relationship between the emission spectra and the low-energy absorption band. These facts are consistent with a small geometry changes between the electronic ground and excited states [12]. The fluorescence maximum is shifted dramatically to longer

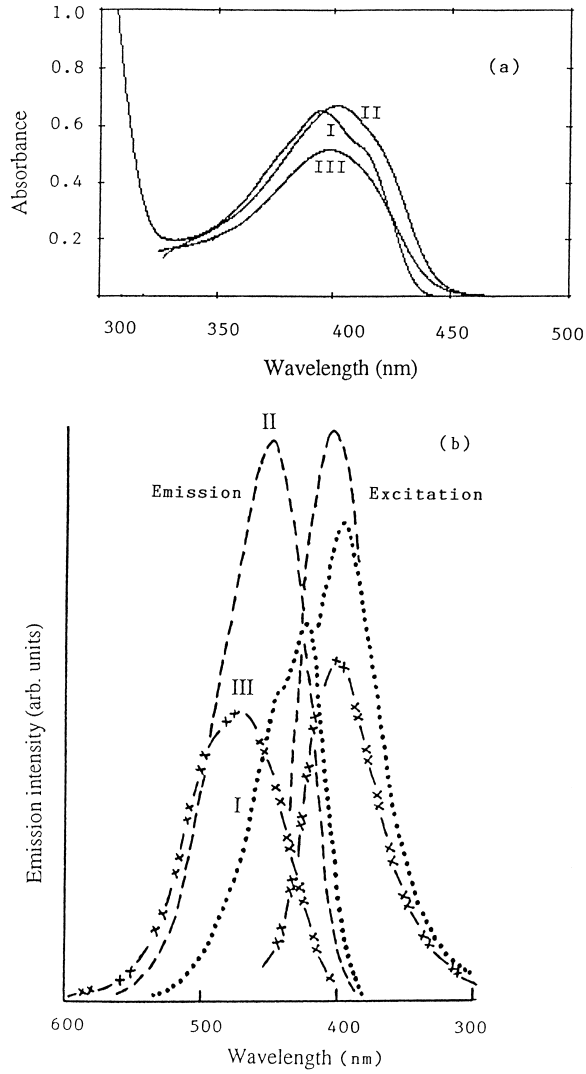

Fig. 1. (a) Electronic absorption spectra and (b) emission and excitation spectra of BQxVB in (I) cyclohexane, (II) DMF and (III) methanol. The excitation spectra were followed at the emission maxima.

Table 1
Spectral properties and the fluorescence quantum yield (ϕ_f) of BQxVB in different organic solvents and microemulsions

Solvent	λ_a^{max}(nm)	$\varepsilon_{max} \times 10^{-4}$ ($M^{-1}\ cm^{-1}$)	λ_f^{max} (nm)			ϕ_f	
			$\lambda_{ex} = 365$ nm	λ_a^{max}	$\lambda_{ex} = 436$ nm	$\lambda_{ex} = 365$ nm	$\lambda_{ex} = 405$ nm
Methanol	396	10.05	484	484	495	0.54	0.32
Ethanol	400	9.82	487	487	495	0.68	0.31
n-Propanol	399	9.90		471		0.69	0.41
n-Butanol	400	13.20		469		0.77	0.46
Ethylene glycol	398	9.69		485		0.33	0.27
DMF	399	9.85		458		0.63	0.41
Acetone	395	8.15		445		0.58	0.37
CH_2Cl_2	397	10.44		450		0.64	0.42
$CHCl_3$	400	9.63	455	455	456, 477[sh]	0.73	0.39
CCl_4	396	11.11		442		0.44	0.29
Cyclohexane	393	12.98	436, 459[sh]	436	436,464[a]	0.33	0.21
W/O	402	10.94		457		0.79	0.39
O/W	402	9.50		461		0.70	0.45

[a] $\lambda_{ex} = 430$ nm.
sh: shoulder.

wavelengths on increasing the solvent polarity, while the position of the absorption maximum suffers a slight red shift as shown in Table 1. The solvent-induced shifts of the emission spectra can be attributed to a large change in the dipole moment of the excited state compared with that of the ground state.

The fluorescence quantum yield (ϕ_f) of BQxVB is highly sensitive to solvent properties. In aprotic solvents, ϕ_f increases dramatically with increasing solvent polarity (expressed in the π^* scale reported by Kamlet [13]) as shown in Fig. 2. This is probably due to a decrease in the non-radiative decay processes caused by a decrease of the vibronic coupling between the lowest $^1(\pi,\pi^*)$ and $^1(n,\pi^*)$ states in this compound. On the other hand, the fluorescence quantum yield decreases with increasing solvent polarity in the case of protic solvents. This effect can be interpreted in terms of efficient internal conversion by extensive vibronic mixing between the close-lying (n,π^*) and (π,π^*) states. In addition, the radiationless internal conversion is enhanced by hydrogen bonding with solvent molecules. The solvent dependence of the fluorescence yield has been also analyzed in terms of two solvent parameters, namely dipolarity/polarizability (π^*) and solvent acidity (α) [13]. In fact, no significant correlation could be obtained on using all solvents ($r = 0.26$), but the data correlate very well when the solvents are divided into two sets as expressed by the following equations:

For protic solvents:

$$\phi_f = 1.305 - 0.927\pi^*(\pm 0.103) - 0.161\alpha(\pm 0.058) \quad (r = 0.985) \quad (1)$$

For aprotic solvents:

$$\phi_f = 0.334 + 0.335\pi^*(\pm 0.012) + 0.195\alpha(\pm 0.079) \quad (r = 0.999) \quad (2)$$

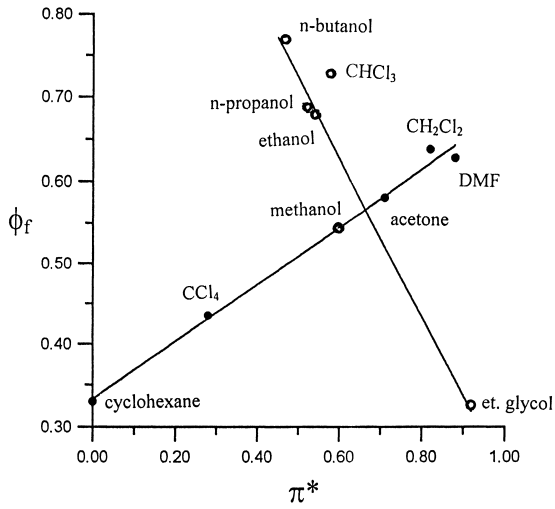

Fig. 2. Plots of ϕ_f vs. π^* values for (●) aprotic solvents and (○) protic solvents.

These findings indicate that the effect of solvent is mainly due to the dipolarity interactions, and support the previously discussed solvent dependence of ϕ_f.

The emission spectra and quantum yields of BQxVB have been also measured in microemulsion media containing chloroform as the oil. Microemulsions have been exploited as media capable of causing molecular dispersion with a subsequent decrease in molecular aggregation and bimolecular reactions [14]. As shown in Table 1, in O/W microemulsion the fluorescence maximum is red shifted ($\lambda_f = 461$ nm) compared with that in W/O and $CHCl_3$ ($\lambda_f = 457$ and 455 nm, respectively). The ϕ_f value in W/O is higher than that in O/W microemulsion ($\phi_f = 0.79$ and 0.70 respectively). However, these values are comparable with the quantum yield measured in bulk chloroform ($\phi_f = 0.73$) indicating that BQxVB is solubilized in the oil phase in both cases. This is confirmed by the close similarity between the emission and excitation spectra recorded in the three media, Fig. 3. The relatively lower ϕ_f value in O/W medium may be due to the quenching role of hydrogen bond formation with the dominant water molecules.

Since the fluorescence spectra of BQxVB are sensitive to the environment, it seems reasonable to study the fluorescence quenching by Fe^{3+} ions in micelles to get information on the micro-environment encountered by solubilized dye molecules. The electronic absorption spectrum of BQxVB in 2% methanolic water shows no changes when $FeCl_3$ is

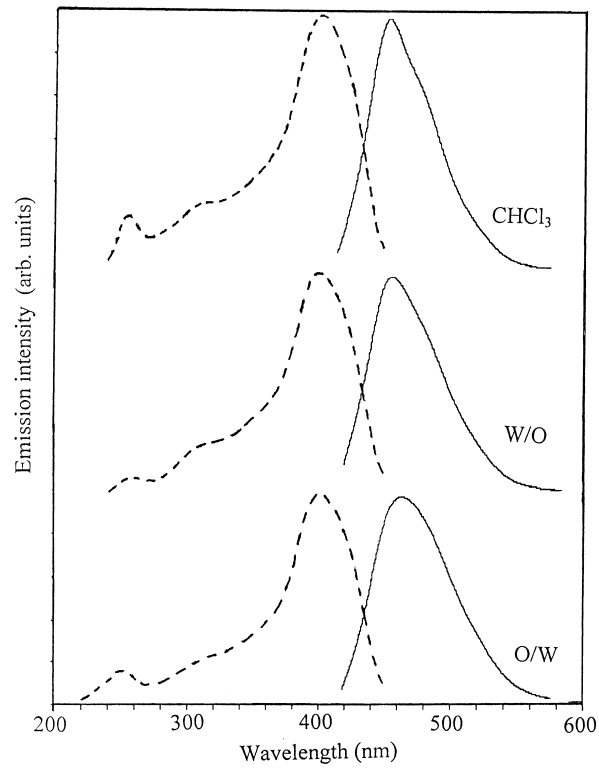

Fig. 3. Emission and excitation spectra of BQxVB in $CHCl_3$, W/O and O/W microemulsions.

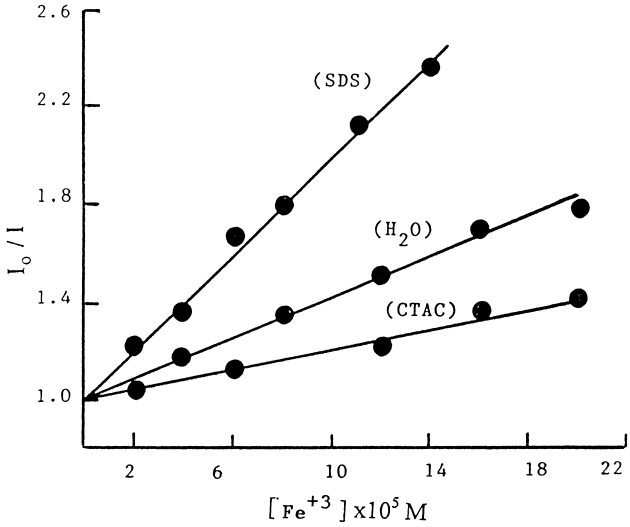

Fig. 4. Stern–Volmer plots for the fluorescence quenching of BQxVB by Fe^{+3} in SDS, water and CTAC micelles.

added, indicating the absence of ground state interactions between BQxVB and Fe^{3+} ions. Also, no discernible changes in that fluorescence maximum or band shape accompanied quenching excluding exciplex formation. The quenching of BQxVB by Fe^{3+} in water as well as cationic (SDS) and anionic (CTAC) micelles follows the Stern–Volmer relation as illustrated in Fig. 4. The quenching constants (K_{SV}) calculated from the slopes of the plots are 9.96×10^3, 4.44×10^3 and $1.92 \times 10^3\ M^{-1}$ in SDS, water and CTAC, respectively. The quenching efficiency in SDS is more than five times higher than that in CTAC micellar solution. This can be explained on the basis of BQxVB solubilization in the micelle phase, however, BQxVB is sparingly soluble in water but becomes soluble in micelles as reflected by the increased fluorescence intensity. In SDS, Fe^{3+} ions become adsorbed on the micelle's surface in the place of the counterion, leading to efficient quencher–fluorescer interactions and thereby enhanced quenching. On the other hand, in CTAC micellar solution, the electrostatic repulsion between the quencher and the positively charged micelle's surface displaces the quencher from the vicinity of the excited BQxVB causing reduction of the quenching efficiency. Since there is no overlap between the absorption spectrum of $FeCl_3$ and the emission spectrum of BQxVB, so quenching via energy-transfer can be neglected. It seems that Fe^{3+} ions quench the fluorescence of BQxVB by charge transfer from the excited BQxVB to the ground state Fe^{3+} ions and/or heavy atom effects.

3.2. Conformational equilibrium of BQxVB

The fluorescence spectra as well as ϕ_f in various solvents varied greatly upon changing the excitation wavelength, see Fig. 5 and Table 1. This was explained in terms of conformational equilibrium [15–17] where for BQxVB at least two conformers are possible due to rotation of both quinoxaline rings around the quasi-single bonds between the ethylenic carbon atoms and the aromatic groups. The emission properties (maxima and quantum yields) indicate the excitation at shorter wavelength (365 nm) populates a conformer which gives short-wavelength fluorescence with higher fluorescence quantum yield. Contrary to this, excitation in the long-wavelength edge of the absorption spectra (436 nm) leads to a conformer which displays long-wavelength fluorescence with lower quantum yield. The fluorescence spectra of BQxVB in cyclohexane at various excitation wavelengths (Fig. 5 (b)) display structure shape with two components, probably the summation of different conformers in equilibrium. On changing the excitation wavelength, the composition of the excited conformers changes and the contribution of each conformer to the fluorescence spectra is different, thus changing the shape of the fluorescence spectra.

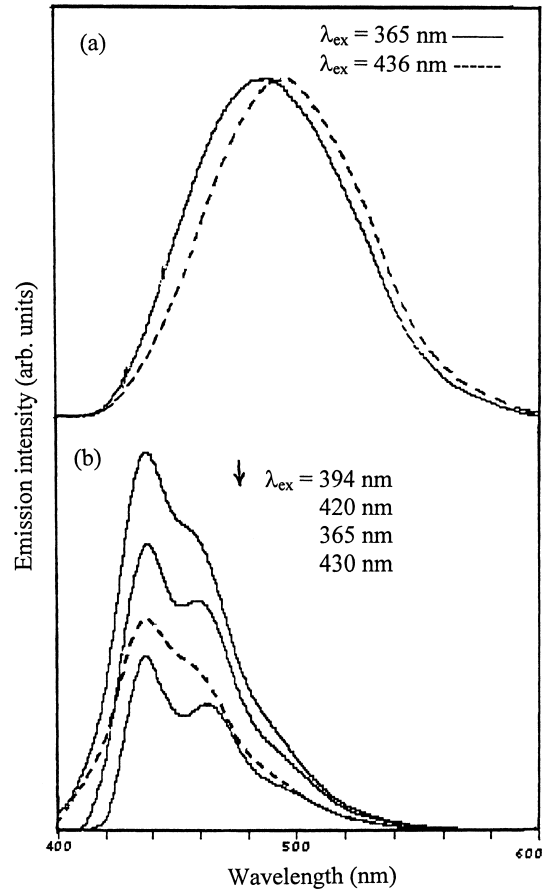

Fig. 5. Emission spectra of BQxVB in (a) methanol and (b) cyclohexane recorded at different excitation wavelengths. The spectra in methanol were normalized to highlight the shift in the maxima.

3.3. Trans⇌cis photoisomerization and photoreactivity of BQxVB in chloromethanes

With the aim of testing whether BQxVB can serve as a laser dye, its photostability has been studied in different

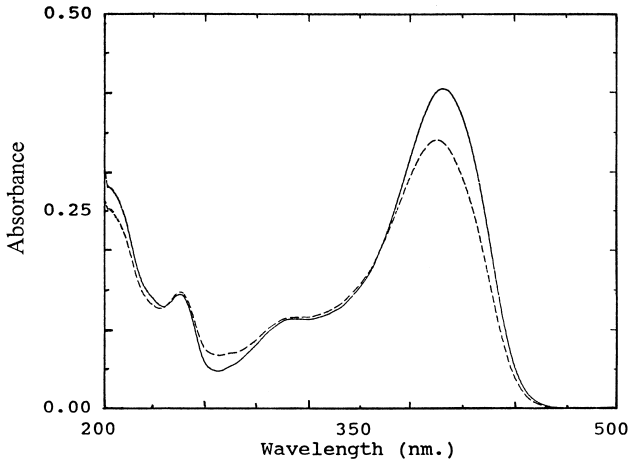

Fig. 6. Absorption spectra of BQxVB in methanol (———) fresh solution and (- - -) photostationary state obtained after irradiation at 405 nm for 45 min.

solvents as well as in microemulsions. Upon irradiation of 5×10^{-6} M BQxVB in methanol at 405 nm, for example, the conversion reaches a photostationary state with the appearance of an isosbestic point at 361 nm, Fig. 6. The photoreaction is assigned to the *trans/cis* photoisomerization since the photostationary state is displaced to the *trans*-rich side on irradiation with shorter wavelength (254 nm) and its absorption maximum is shifted to shorter wavelength compared to the pure *trans* isomer. The photochemical quantum yields ($\phi_{t\rightarrow c}$) of the *trans* → *cis* isomerization as well as the composition of the photostationary states (expressed as *%cis*) have been measured using two different excitation wavelength and the data are summarized in Table 2. Both $\phi_{t\rightarrow c}$ and the *%cis* are sensitive to the medium and excitation wavelength. As can be seen from the data in Tables 1 and 2, the decrease in the fluorescence yield is accompanied by an increase in the photochemical quantum yield. This indicates that the *trans* → *cis* photoisomerization proceeds through an excited state similar to the fluorescing state. The larger excitation wavelength effect on the photoisomerization quantum yield is a further indication for the previously discussed conformational equilibrium of BQxVB. The lower photochemical quantum yields and appearance of *trans*-rich photostationary states reflect a reasonable photostability of BQxVB with respect to UV light. Thus, it can serve as an effective laser dye.

Table 2
Quantum yields of *trans* → *cis* photoisomerization and the percentage of the *cis* isomer measured at two irradiation wavelengths in different solvents

Solvent	$\lambda_{irr} = 382$ nm		$\lambda_{irr} = 405$ nm	
	$\phi_{t\rightarrow c}$	*%cis*	$\phi_{t\rightarrow c}$	*%cis*
Methanol	0.005	10	0.008	18
DMF	0.003	8	0.006	16
$CHCl_3$	0.004	7	0.005	16
Cyclohexane	–	0.6	0.001	5
W/O	–	22	0.008	32
O/W	0.003	17	0.006	29

However, BQxVB undergoes photodecomposition in chloromethane solvents such as CCl_4, $CHCl_3$ and CH_2Cl_2 upon irradiation at 254 nm, Fig. 7. The absorbance of the band around 400 nm decreases with increasing the irradiation time. Also, the photoproduct displays a distinct absorption band around 460 nm in the case of $CHCl_3$ and CH_2Cl_2 but is missed in CCl_4. Furthermore, the photoproduct gives strong emission at ca. 500 nm as shown in Fig. 8.

The rate constants of the photodecomposition of BQxVB were calculated by applying the simple first-order kinetics and were found to be 0.037, 0.011 and 0.001 s^{-1} in CCl_4 ($E_A = 2.12$ eV), $CHCl_3$ ($E_A = 1.75$ eV) and in CH_2Cl_2 ($E_A = 1.36$ eV) [18], respectively. It could be easily observed that the rate constant increases with increasing

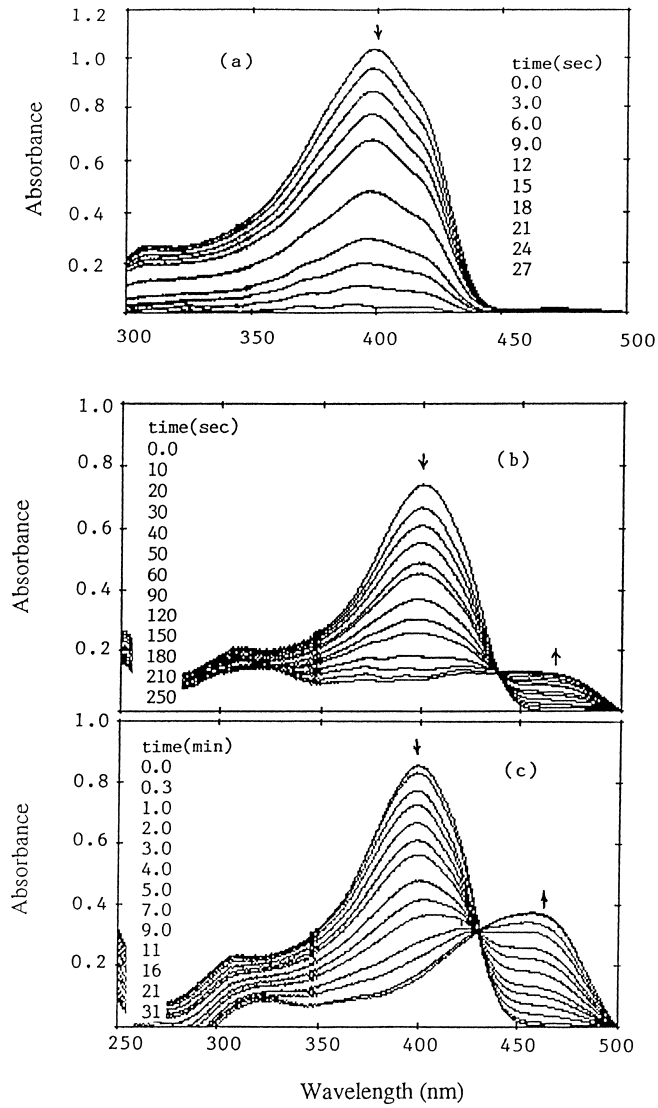

Fig. 7. Effect of photoirradiation at 254 nm ($I_o = 4.2 \times 10^{-6}$ Ein/min) on the absorption spectra of BQxVB in (a) CCl_4 (b) $CHCl_3$ and (c) CH_2Cl_2. Time of irradiation is indicated on each run.

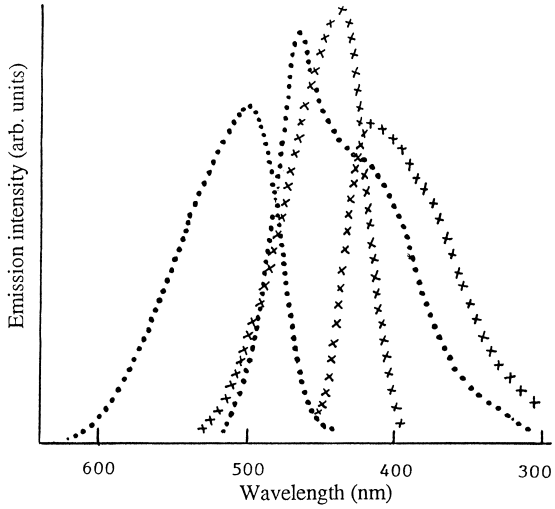

Fig. 8. Emission and excitation spectra of BQxVB in CH_2Cl_2 (× × ×) before irradiation and (. . .) after irradiation at 254 nm for 31 min.

the electron affinity (E_A) of the solvent. This result indicates that the photodecomposition of BQxVB proceeds via an electron transfer step from excited $BQxVB^*$ to the solvent molecules.

The photodecomposition of BQxVB in chloromethanes can be explained according to the reaction scheme proposed to account for the photoreactions of carbolines [18] in $CHCl_3$ and CCl_4:

$$BQxVB + h\nu \rightarrow^2 [BQxVB]^* \quad \text{light absorption} \quad (3a)$$

$$^2[BQxVB]^* \rightarrow^1 [BQxVB]^* \quad \text{internal conversion} \quad (3b)$$

$$^1[BQxVB]^* \rightarrow BQxVB + h\nu_{fluo} \quad (3c)$$

$$^1[BQxVB]^* + CH_nCl_{4-n} \rightarrow [BQxVB^{\delta+} \cdots ^{\delta-} CH_nCl_{4-n}]^* \quad \text{exciplex} \quad (3d)$$

$$[BQxVB^{\delta+} \cdots ^{\delta-} CH_nCl_{4-n}]^* \rightarrow [BQ \times VB^{\bullet+} \cdots ^{\bullet-} CH_nCl_{4-n}] \quad \text{electron transfer} \quad (3e)$$

$$[BQxVB^{\bullet+} \cdots ^{\bullet-} CH_nCl_{4-n}] \rightarrow [BQxVB^{\bullet+} \cdots Cl^- \cdots CH_nCl_{3-n}] \quad (3f)$$

The formation of the chloride ion in the contact ion pair, step (3f) was tested by using an ethanolic $AgNO_3$ solution where a white precipitate from AgCl was formed. The photodecomposition of some diolefinic dyes [19] and anthracene laser dyes [20] have been recently examined. The photoionization of some aromatic and aliphatic amines in CCl_4, $CHCl_3$ and CH_2Cl_2 has also been reported [21].

3.4. Laser activity and excitation energy transfer

The laser action of BQxVB solution (ca. 10^{-3} mol dm^{-3}) has been studied in DMF solvent in which $\phi_f = 0.63$ ($\lambda_{ex} = 365$ nm) and the photochemical quantum yield is very low ($\phi_{t\rightarrow c} = 0.003$). On pumping BQxVB solution in DMF using nitrogen laser pulses ($\lambda_{ex} = 337.1$ nm) of 800 ps duration and 1.48 mJ pulse, the dye gives laser emission in the range 440–485 nm with a maximum laser emission at 460 nm. The output energy of laser dye was measured by a power meter as a function of the wavelength to determine the lasing range. The maximum gain coefficient (α) was calculated ($\alpha = 2.3\ cm^{-1}$) at the maximum laser emission (460 nm) by measuring the intensity I_L of laser emission from the entire cell length L and the intensity $I_{L/2}$ from the cell half length, according to the following relation [22]:

$$\alpha = \frac{2}{L} \ln\left[\frac{I_L}{I_{L/2}} - 1\right] \quad (3)$$

The cross section for stimulated laser emission (σ_e) was calculated at the emission maximum according to the equation [23]:

$$\sigma_e = \frac{\lambda_e^4 E(\lambda)}{8\pi c_o n^2} \times \frac{\phi_f}{\tau_f} \quad (4)$$

where λ_e is the emission wavelength, n the refractive index of the medium, c_o the velocity of light and $E(\lambda)$ the normalized fluorescence line-shape function where

$$\int_0^\infty E(\lambda)d\lambda = \phi_f \quad (5)$$

for BQxVB $\tau_f = 1.1$ ns in DMF and σ_e=3.11 × 10^{-16} cm^2 at 460 nm.

It is worth mentioning here that BQxVB acts as a good energy donor for laser dyes which have low molar absorptivities at 337.1 nm (nitrogen laser) such as rhodamine B (RB). An equimolar mixture of BQxVB and RB in ethanol gives laser emission in the spectral range of RB (600–650 nm) upon excitation by nitrogen laser pulses. This indicates excitation energy transfer from excited BQxVB to RB. The sensitized RB fluorescence was observed in the presence of BQxVB. As shown in Fig. 9 (a), the fluorescence intensity of RB, measured at 570 nm where BQxVB has no emission, increases with increasing the concentration of BQxVB.

The fluorescence quenching of BQxVB has also been studied in ethanol using RB as a quencher to determine the rate constant of energy transfer (k_{ET}) in BQxVB/RB system. k_{ET} can be calculated by applying the Stern–Volmer relation in the form [24]

$$\frac{I_o}{I} = 1 + k_{ET}\tau_f[Q] \quad (6)$$

where I_o and I are the fluorescence intensities in the absence and presence of the accepted concentration [Q] and τ_f is the fluorescence lifetime of BQxVB (=1.7 ns in ethanol). From the fluorescence lifetime and the slope of the Stern–Volmer plot, (Fig. 9 (b)), k_{ET} has been calculated as 16.2 × 10^{12} M^{-1} s^{-1}. This value is much higher than the diffusion rate constant in ethanol ($d_{diff} = 9.2 \times 10^9$ M^{-1} s^{-1}

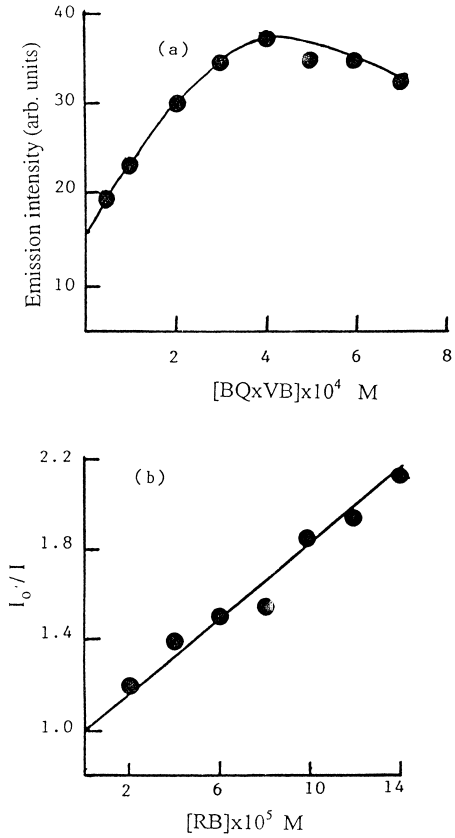

Fig. 9. (a) Emission intensity of RB followed at 570 nm vs. concentration of BQxVB in ethanol ($\lambda_{ex} = 337$ nm). (b) Stern–Volmer plot of fluorescence quenching of BQxVB by RB in ethanol.

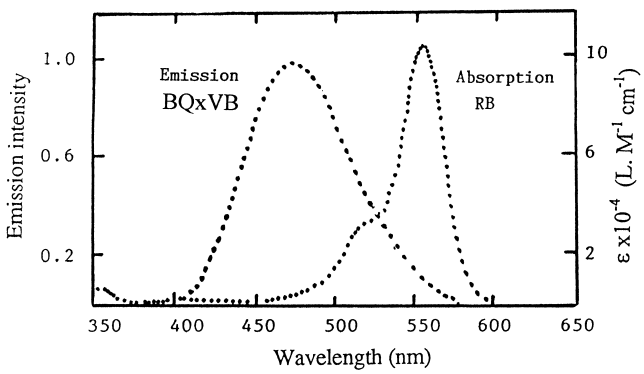

Fig. 10. Overlap between the emission spectrum of BQxVB and the absorption spectrum of RB in ethanol.

at 25°C). There is a significant overlap between the electronic absorption spectrum of RB and the emission spectrum of BQxVB. Fig. 10. Applying Forster's resonance energy transfer mechanism, the critical transfer distance (R_o) for the BQxVB/RB system can be calculated [25].

$$R_o^6 = \frac{1.25 \times 10^{-25} \times \phi_f}{n^4} \int_0^\infty \frac{F_D \varepsilon(\bar{\nu}) d\bar{\nu}}{\bar{\nu}^4} \quad (7)$$

where R_o is the distance at which energy transfer and emission process are equally probable (critical transfer distance). ϕ_f is the emission quantum yield of the donor, n the refractive index of the solvent and the integral is the overlap integral for fluorescence spectrum of the donor normalized to unity (F_D) and absorption spectrum of the acceptor (ε_A). Accordingly, the critical transfer distance was calculated as 31.3 Å. This value is higher than that for collisional energy transfer in which $R_o < 10$ Å [26]. The high value of the critical transfer distance as well as the energy transfer within the BQxVB/RB pair is a resonance energy transfer due to long range dipole–dipole interaction between the excited donor and the ground state acceptor.

Acknowledgements

We thank Prof. Dr. G. Grampp and Dr. S. Landgraf, Institute of Physical and Theoretical Chemistry, TU-Graz, Austria for providing the facilities for lifetime measurements.

References

[1] E.M. Ebeid, M.M.F. Sabry, S.A. El-Daly, Laser Chem. 5 (1985) 223.
[2] E.M. Ebeid, R.M. Issa, S.A. El-Daly, M.M.F. Sabry, J. Chem. Soc., Faraday Trans. 2(82) (1986) 1981.
[3] S.A. El-Daly, S.M. Al-Hazmy, E.M. Ebeid, E.M. Vernigor, J. Photobiol. A: Chem. 91 (1995) 199.
[4] S.A. El-Daly, S.M. Al-Hazmy, E.M. Ebeid, A.C. Bhasikuttan, D.K. Palit, A.V. Spare, J.P. Mittal, J. Phys. Chem. 100 (1996) 9732.
[5] S.A. El-Daly, E.M. Ebeid, S.M. El-Hazmy, A.S. Babaqi, Z. El-Gohary, G. Duportail, Proc. Indian Acad. Sci. (Chem. Sci.) 105 (1993) 651.
[6] S.A. El-Daly, T.A. Fayed, Spectrochim. Acta A: (1999) accepted for publication.
[7] J.K. Landquist, G.J. Stacey, J. Chem. Soc., (1953) 2822.
[8] E.M. Ebeid, M.H. Abdel-Kader, M.M.F. Sabry, A.B. Yousef, J. Photochem. Photobiol. A: Chem. 44 (1988) 153.
[9] J.V. Morris, M.A. Mahaney, J.R. Huber, J. Phys. Chem. 80 (1976) 969.
[10] I.G. Hatchard, C.A. Parker, Proc. Royal Soc. London, Ser. A. 235 (1959) 518.
[11] G. Gauglitz, J. Photochem. 5 (1976) 41.
[12] T.D.Z. Atvaes, C.A. Bortolato, D. Dibbern Brunelli, J. Photochem. Photobiol. A: Chem. 68 (1992) 41.
[13] M.J. Kamlet, J.M. Abboud, M.H. Abraham, R.W. Taft, J. Org. Chem. 48 (1983) 2877.
[14] J.H. Fendler, J. Phys. Chem. 84 (1980) 1485.
[15] U. Mazzucato, Pure Appl. Chem. 54 (1982) 1705.
[16] S.C. Shim, K.T. Lee, M.S. Kim, J. Org. Chem. 55 (1990) 4316.
[17] B.M. Jeong, S.C. Shim, J. Photochem. Photobiol. A: Chem. 79 (1994) 39.
[18] M.C. Biondic, R. Erra-Balsells, J. Photochem. Photobiol. A: Chem. 77 (1994) 149.
[19] S.A. El-Daly, Monatshefte fur Chemie 129 (1998) 835.
[20] S.A. Azim, H.A. El-Daly, S.A. El-Daly, Kh.A. Abou-Zeid, E.M. Ebeid, J.R. Heldt, J. Chem. Soc., Faraday Trans. 92 (1996) 2685.
[21] A.J. Bard, A. Ledwith, H.J. Shine, Adv. Phys. Org. Chem. 12 (1976) 155.

[22] J.C. delValle, M. Kasha, J. Catalan, J. Phys. Chem. A 101 (1997) 3260.
[23] M. Rink, H. Gusten, H.J. Ache, Phys. Chem. 90 (1986) 2661.
[24] G.R. Penzer, in: S.B. Brown (Ed.), An Introduction to Spectroscopy for Biochemists, Academic Press, London, 1980, p. 86.
[25] A. Gilbert, J. Baggott (Eds.), Essentials of Molecular Photochemistry, Blackwell, London, 1991, p. 186.
[26] S.G. Schulman, Modern Fluorescence Spectroscopy, in: E.L. Wehry (Ed.), Plenum Press, New York, 1976, vol. 2.